The Restitution Portrait: A New Method for Investigating Rate-Dependent Restitution

SOMA S. KALB, M.S.E.,* HANA M. DOBROVOLNY, M.S.,† ELENA G. TOLKACHEVA, PH.D.,† SALIM F. IDRISS, M.D., PH.D.,*,‡ WANDA KRASSOWSKA, PH.D.,* and DANIEL J. GAUTHIER, PH.D.*,†

From the Departments of *Biomedical Engineering and †Physics, and Center for Nonlinear and Complex Systems, Duke University, and ‡Pediatric Cardiology, Duke University Medical Center, Durham, North Carolina, USA

The Restitution Portrait. ***Introduction:*** **Electrical restitution, relating action potential duration (APD) to diastolic interval (DI), was believed to determine the stability of heart rhythm. However, recent studies demonstrate that stability also depends on long-term APD changes caused by memory. This study presents a new method for investigation of rate- and memory-dependent aspects of restitution and for assessment of mapping models of APD.**

Methods and Results: **Bullfrog ventricular myocardium was paced with a "perturbed downsweep protocol." Starting from a basic cycle length (BCL) of 1,000 ms, the tissue was paced until steady state was achieved, followed by single beats of longer and shorter cycle lengths. BCL was decreased by 50 to 100 ms and the process repeated. All APDs were plotted as a function of the preceding DI, which allowed simultaneous observation of dynamic, S1-S2, and two constant-BCL restitution curves in a "restitution portrait." Responses were classified as 1:1 (stimulus:response), transient 2:2, or persistent 2:2 (alternans) and were related to the slopes of the restitution curves. None of these slopes approached unity for the persistent 2:2 response, demonstrating that the traditional restitution condition does not predict alternans. The restitution portrait was used to evaluate three mapping models of APD. The models with no memory and with one-beat memory did not produce restitution portraits similar to the experimental one. A model with two-beat memory produced a qualitatively similar portrait.**

Conclusion: **The restitution portrait allows a more comprehensive assessment of cardiac dynamics than methods used to date. Further study of models with memory may result in a clinical criterion for electrical instability.** *(J Cardiovasc Electrophysiol, Vol. 15, pp. 698-709, June 2004)*

dynamic, S1-S2, constant basic cycle length, restitution, memory, alternans, action potential duration, stability, mapping model

Introduction

One of the most fundamental characteristics of cardiac cells is the shortening of the action potential duration (APD) as the heart rate increases, known as *electrical restitution*. Restitution plays a vital role in heart function: for a given heart rate, a shorter APD allows for a longer diastolic interval (DI), thereby giving adequate time for the heart to refill with blood. Although important for life at moderate heart rates, restitution can give rise to life-threatening rhythms for fast rates. For example, it was observed nearly a century ago[1] that small pieces of paced myocardium displayed a phase-locked 1:1 response pattern for slow pacing, which was often replaced by a 2:2 pattern (alternans) as the pacing rate increases. Furthermore, analyses of mathematical models of the whole heart suggest that alternans can trigger the onset of fibrillation.[2] Consistent with these findings, recent clinical studies have shown a correlation between electrical alternans in the ECG and vulnerability to fibrillation.[3-5]

Because of the possible link between alternans and fibrillation, numerous studies have investigated restitution and its role in destabilizing the 1:1 response pattern. Early work suggested that the transition to alternans can be understood by analyzing the nonlinear functional relationship between the APD and the preceding DI, known as the *restitution relation* or *restitution curve*. It was proposed that the 1:1 state becomes unstable when the absolute value of the slope of the restitution curve exceeds one,[6,7] hereafter referred to as the *restitution condition*. This condition has been confirmed in some experiments[8] and modeling studies[2,9] and has led to the hypothesis that flattening the restitution curve will help prevent fibrillation. Recent experiments have indicated that fibrillation can be suppressed using pharmacologic agents that reduce restitution slope,[10] leading some to suggest that the restitution slope is a promising target for antiarrhythmia drug design.[11,12]

This pioneering early work is the basis for our intuitive understanding of the origin of alternans and the resulting restitution condition is firmly ingrained in the minds of most researchers and clinicians. However, there is a considerable body of research demonstrating that this condition is incorrect in many situations,[13] where stable 1:1 behavior is observed when the restitution curve is very steep (slope >1)[14,15] or 2:2

This work was supported by National Science Foundation Grant PHY-0243584 and National Institutes of Health Grant 1RO1-HL-72831.

Address for correspondence: Soma S. Kalb, M.S.E., Department of Biomedical Engineering, Box 90281, Duke University, Durham, NC 27708. Fax: 919-660-5405; E-mail: ss49@duke.edu

Manuscript received 5 October 2003; Accepted for publication 29 December 2003.

doi: 10.1046/j.1540-8167.2004.03550.x

behavior is seen for a shallow curve (slope < 1).[16] In addition, many experiments have shown that the mathematical model on which the hypothesis is based is incomplete: the restitution curve has been shown to depend on the manner in which it is measured,[17] suggesting that APD is a function of more than just the preceding DI, a concept known as "memory." Note that in this article, the term "memory" refers to the APD changes occurring on the time scale of minutes rather than the changes in T wave configuration occurring on the time scale of hours or days after altered activation, also called memory.[18]

Recently, memory has been incorporated in mathematical models,[19–24] and analysis of such models has explained the possible origins of different restitution curves.[21,24] Two commonly measured restitution curves are the S1-S2 and dynamic restitution curves. In an S1-S2 restitution protocol, a premature stimulus (S2) is applied at various times relative to the end of a series of paced (S1) beats. In a dynamic restitution protocol, steady-state APD and preceding DI are measured as basic cycle length (BCL) is decreased. A less-known restitution curve is the constant-BCL (CB) restitution curve,[16,21,24] where APD and preceding DI pairs are measured for a given BCL, both steady state and transient. Recent theoretical studies[21,24] have demonstrated the potential importance of the slope of CB restitution curve in determining stability of the 1:1 response for certain models of APD dynamics. However, only recently was a protocol proposed to generate this curve in experiments.[24] Theoretical studies[24] have shown that each of these curves captures a different aspect of restitution dynamics. The S1-S2 restitution curve is a measure of the immediate response to a change in BCL. In contrast, the dynamic restitution curve is a measure of the steady-state response. The CB restitution curve is a measure of the transient response connecting the previous two.

The primary purpose of this study is to use a new pacing protocol to measure simultaneously multiple aspects of cardiac restitution: the steady-state response, the transient response to a perturbation, and long-term accommodation of the response. We use this *perturbed downsweep* protocol, which is a modified version of the protocol proposed by Tolkacheva et al.,[24] to measure the response of small pieces of paced bullfrog ventricular myocardium and visualize all the observed responses in a *restitution portrait*. We use the portrait to assess three different mathematical models of cardiac dynamics: the traditional model that relates the APD to the preceding DI,[7] a model introduced by Otani and Gilmour[21] that relates the previous APD to both the preceding DI and APD, and a model introduced by Chialvo et al.[20] that displays long-term accommodation of the APD.

We find that our observations do not support the restitution condition and that none of the models accurately describes the stability of the 1:1 response pattern. The model displaying long-term accommodation does agree qualitatively with our observations, suggesting that further refinements of this model may lead to a more accurate method for predicting the vulnerability for alternans and hence possibly for fibrillation. Our conclusions are made possible by the unified framework provided by the restitution portrait, demonstrating that it is a powerful new tool for investigating the multidimensional aspects of the response of cardiac tissue while maintaining the simplicity of the restitution concept.

Methods

Six bullfrog (Rana catesbeiana) hearts were studied. Small pieces of ventricular myocardium ($<3 \times 3 \times 5$ mm) were prepared as described previously.[14] Thirty-nine trials were performed (N = 6, 8, 4, 6, 11, and 4 for the six frogs).

Action Potential Recordings

Transmembrane voltage was measured using standard pulled glass microelectrodes filled with 3 mol/L KCl and impaled 1 to 2 mm from the pacing site. In one preparation, 10 mmol/L diacetyl monoxime (DAM) was added to the superfusate to reduce motion and loss of microelectrode impalement. At this concentration of DAM, we did not observe shortening of APD in our preparations, although it was only used when necessary. The tissue, quiescent without pacing, was stimulated with 2-ms rectangular pulses at twice diastolic threshold by a computer-controlled stimulator through a bipolar insulated silver electrode at an initial BCL of 1,000 ms. A custom-written LabView program (National Instruments Corp., Austin, TX, USA) controlled both stimulation and data collection. Electrical signals were low-pass filtered with analog circuitry and acquired at a rate of 1 kHz.

Pacing Protocol

The perturbed downsweep protocol used in this study is a modified version of that proposed by Tolkacheva et al.[24] Starting with a long BCL $= B_0$, typically 1,000 ms, the tissue was paced with decreasing BCL (downsweep). In the figures and throughout this article, the APD and preceding DI pair (DI_n, APD_{n+1}) obtained at BCL $= B$ is denoted R_X^B, where X indicates the type of response. For each BCL $= B$ in the downsweep, six steps were performed (Fig. 1): (I) Stimuli were applied to the tissue at B for 60 seconds to ensure that steady state was achieved. The transient responses from this initial pacing are denoted R_{CB-D}^B. (II) After 60 seconds of pacing at B, 5 to 10 additional stimuli were applied at B to measure the steady-state response. The responses from these five stimuli are denoted R_*^B and represent the steady-state response or *fixed point*. (III) A stimulus was applied at a long coupling interval of $B_L = B + \delta$, where δ typically was 50 ms. The ensuing response is denoted R_L^B. (IV) Pacing at B was resumed for 5 to 10 beats. The responses to these stimuli are denoted R_{CB-S}^B. (V) A stimulus was applied at a short coupling interval of $B_S = B - \delta$, with the ensuing response denoted R_S^B. (VI) Five to 10 more stimuli were applied at B, with responses also denoted R_{CB-S}^B. The BCL was decremented by Δ (typically 50–100 ms), and steps I–VI were repeated until a 2:1 response occurred. At each BCL, transmembrane potential was recorded for the first 20 to 40 seconds of step I and for all responses in steps II to VI.

Determination of Restitution Curves

Restitution curves were generated off-line using Matlab software (MathWorks, Inc., Natick, MA, USA). The APD and preceding DI were measured at 70% repolarization. The resulting responses R_X^B, as described earlier, were fit to appropriate functions to yield dynamic, S1-S2, and CB restitution curves as shown in Figure 1 and described as follows.

The dynamic restitution curve is composed of the steady-state responses R_*^B over all B in the downsweep, as indicated by a "D" in Figure 1. To determine the slope of the curve,

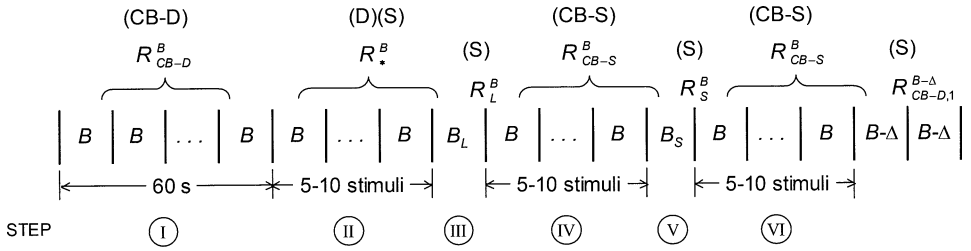

Figure 1. *Sequence of stimuli applied at each basic cycle length (BCL) in the downsweep. B is the downsweep BCL. $B_L = B+\delta$ and $B_S = B-\delta$. $B - \Delta$ is the next BCL in the downsweep. Notation for responses to stimuli is shown above the appropriate stimulus train, where R_X^B represents the (DI_n, APD_{n+1}) pair for that stimulus. The responses are used to generate the restitution curves shown in the top line (parentheses): CB restitution curves (CB-D and CB-S), dynamic restitution curve (D), and S1-S2 restitution curve (S). See text for details.*

these points were fit to an exponential of the form:

$$APD = a - be^{-DI/\tau}. \quad (1)$$

Whereas the dynamic restitution curve consists of one curve over all BCLs, the perturbed downsweep protocol yields small segments of CB and S1-S2 restitution curves for each BCL. In our experiments, CB restitution consisted of two components: those responses obtained from step I in the pacing protocol (R^B_{CB-D}) and those responses from steps IV and VI (R^B_{CB-S}). These two components fell in two different loci and were fit separately to form two restitution curves, CB-D ("D" for *dynamic transient*) and CB-S ("S" for *S1-S2 transient*) for each BCL. At a given B, responses R^B_{CB-D} and R^B_{CB-D} were both fit to lines of the form:

$$APD = S_{CB}DI + b \quad (2)$$

by least squares linear regression. This form was chosen after examining R^B_{CB-S} and R^B_{CB-D} data obtained from preliminary experiments. As shown in the Results section, this choice is readily apparent for the CB-D restitution. The CB-S responses result from brief perturbations to BCL, where the transient response quickly returns to steady state and does not offer many points from which to ascertain the functional form. For this reason, a local slope is determined by linear regression.

To generate the S1-S2 restitution curve at a given B, four points were used as shown in Figure 1: $R^{B-\Delta}_{CB-D,1}$, R^B_S, R^B_*, and R^B_L, where $R^{B-\Delta}_{CB-D,1}$ is the response to the first stimulus at the next BCL in the downsweep. In conventional terms, these responses were collected with an S1-S1 coupling interval equal to B and with S1-S2 coupling intervals equal to (B-Δ), B_S, B, and B_L, from shortest to longest. Thus, these four points form a segment of a traditional S1-S2 restitution curve, where the S1-S1 interval equals B. To compute the slope of this curve, these points were fit to an exponential of the form of Equation 1, and the slope was determined analytically at the desired DI.

Results

Restitution Curves at a Single BCL in the Downsweep

Figure 2 shows an example of typical responses at one BCL ($B = 550$ ms) for an experiment where $B_0 = 950$ ms, $\Delta = 100$ ms, and $\delta = 50$ ms. Following the decrease in BCL from 650 to 550 ms, the points labeled CB-D show the restitution response R^{550}_{CB-D} resulting from the initial 60 seconds of pacing (of which only the first 20 seconds are shown). After an initial excursion labeled as "1" in Figure 2, the CB-D responses fell on the line $APD_{n+1} + DI_n = 550$ ms. Hereafter, this line $APD_{n+1} + DI_n = BCL$ is referred to as the *BCL-line*. During this initial pacing, APD decreased (DI increased).

When an R_{CB-D} response is plotted versus time, APD shows a fast jump followed by a slower exponential decay with a time constant of approximately 20 seconds (Fig. 3). The slow change in APD that follows a fast change in APD has been termed *accommodation* by Watanabe and Koller.[22] It has been reported in ventricular preparations of many species including dog,[22] cat,[25] rabbit,[26] guinea pig,[27] sheep,[27] and human.[28] The time constants reported therein are comparable to that observed in our preparation, indicating that the temporal dynamics of the bullfrog preparation is similar to other species. This observed accommodation demonstrates the need for at least a full minute of pacing at a given BCL to reach steady state.

After 60 seconds, the steady-state response R^{550}_*, denoted "2" in Figure 2, was attained and plotted as point on the dynamic restitution curve. After the stimulus at B_L was applied, its response R^{550}_L yielded one point of the S1-S2 restitution curve ("3" in Fig. 2). When pacing at B was resumed, APD and DI initially oscillated ("4" in Fig. 2) before returning to steady state. These R^{550}_{CB-S} responses formed part of the CB-S restitution curve. The response R^{550}_S to the second perturbation at B_S yielded another point of the S1-S2 restitution

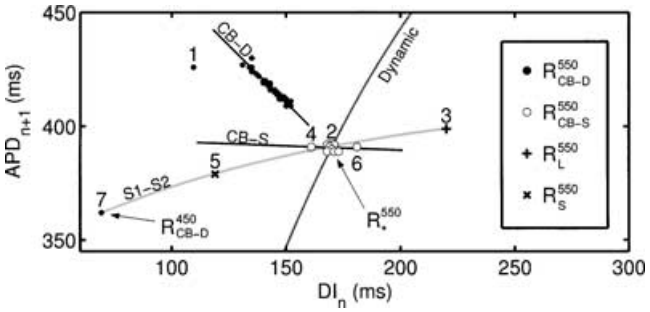

Figure 2 *Restitution curves at a single basic cycle length (BCL) of 550 ms. The filled circles represent the DI_n, APD_{n+1} pairs resulting from step I of the pacing protocol (only the first 20 seconds are shown). These form the CB-D restitution curve. After 60 seconds, the steady-state response, R^{550}_* (point 2), is denoted as a point on the dynamic restitution curve. The responses to the long perturbation R^{550}_L (point 3), the short perturbation R^{550}_S (point 5), R^{550}_*, and the first point at the new BCL (7) constitute the S1-S2 restitution curve. The responses after both perturbations (open circles) constitute the CB-S restitution curve. Lines fit through the various responses form the restitution curves as labeled on the plot.*

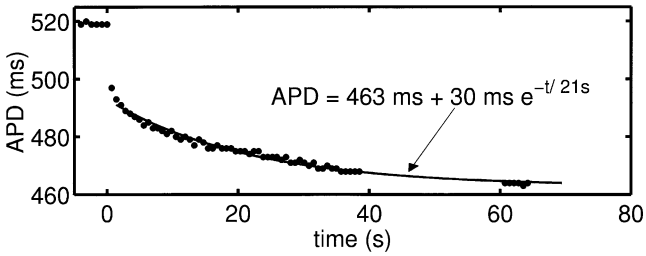

Figure 3. *Action potential duration (APD) accommodation after a change in basic cycle length (BCL). After a decrease in BCL, APD shows an initial fast jump (at time = 0 seconds). APD then decreases slowly with an exponential time course. The filled circles beginning at time = 0 seconds represent the data recorded during step I of the protocol. Forty of 60 seconds are recorded. The filled circles beginning at time = 60 seconds are the data recorded during step II of the protocol. The solid line shows an exponential of the form APD = a +bexp(–DI/τ) fit to the slow change in APD.*

curve ("5" in Fig. 2). The stimuli following short perturbation also yielded an initially oscillating response ("6" in Fig. 2), which then returned to steady state. The beats following the short perturbation are also R^{550}_{CB-S} responses and constitute the remaining points used to form the CB-S restitution curve. The point labeled "7" was the first response at the new BCL ($B - \Delta = 450$ ms), $R^{450}_{CB-D,1}$. This point, along with R^{550}_{S}, R^{550}_{*}, and R^{550}_{L}, constitutes the S1-S2 restitution curve. Note that the S1-S2 restitution curve is only a segment of the conventional S1-S2 restitution curve for a small range of DI around the fixed point in this protocol.

Classification of Responses

The responses to a sustained change in BCL (R^{B}_{CB-D}), as shown by the CB-D restitution curves, were classified into one of four categories: 1:1, transient 2:2 (2:2T), persistent 2:2 (2:2P), or complex. At a given BCL, $\Delta APD_n = APD_n - APD_{n+1}$ was determined for all CB-D data points and plotted versus time (Fig. 4).The 1:1 responses were categorized as

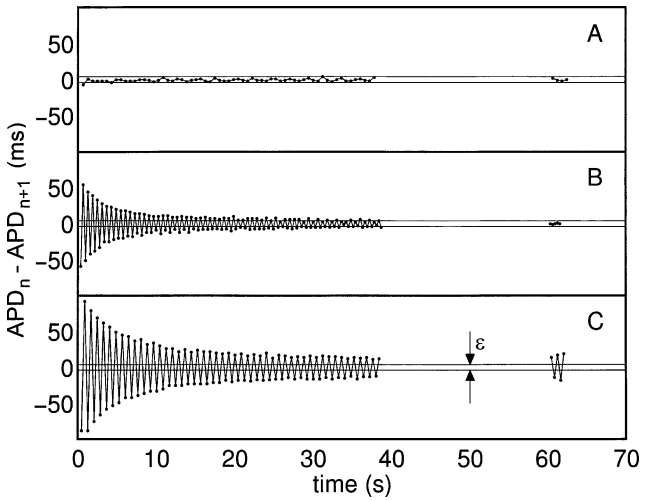

Figure 4. *Classification of responses: (A) 1:1 responses, (B) 2:2T responses, (C) 2:2P responses. Data shown was obtained during steps I and II of the perturbed downsweep protocol. As shown in panel C, horizontal lines indicate $APD_n - APD_{n+1} = \pm\varepsilon$, the experimental error.*

those responses where $|\Delta APD_n|$ exceeded the experimental error in determining ΔAPD_n (error, $\varepsilon = 4$ ms) for less than 10 beats (Fig. 4A). The 2:2 responses consisted of those responses where ΔAPD_n changed in sign from beat to beat and $|\Delta APD_n| > \varepsilon$ for more than 10 beats. If $|\Delta APD_n|$ decreased and remained below ε during step I of the protocol, the response was categorized as 2:2T (Fig. 4B). If $|\Delta APD_n|$ remained above ε for the duration of step I, the response was 2:2P (Fig. 4C). If ΔAPD_n did not show an alternating pattern with $|\Delta APD_n| > \varepsilon$, the response was categorized as complex. This classification was performed for every BCL in all trials. Over all BCLs, trials, and preparations, there were 267 1:1 responses, 20 2:2T responses, 16 2:2P responses, and 6 complex responses. The complex responses were excluded from the following analysis.

Restitution Portrait: 1:1 Responses

Figure 5 shows the restitution curves at all BCLs in the downsweep showing a 1:1 response for the same trial as that shown in Figure 2 for a single BCL. A set of restitution curves similar to Figure 2 is seen at each BCL, starting with BCL = 950 ms at the top. We call this collection of restitution curves the *restitution portrait*. The set of steady-state responses makes up the dynamic restitution curve. The slope of the dynamic restitution curve S_{dyn} was >1 for all BCLs <850 ms, reaching a value of 3.3 at BCL = 250 ms before the response switched to 2:1. At each BCL, the first few CB-D responses oscillated before falling onto the line of slope nearly equal to –1. This oscillation was more pronounced at lower BCLs. At each BCL, there is a different S1-S2 restitution curve due to rate-dependent restitution. For all BCLs, the S1-S2 restitution curve remained relatively flat but grew

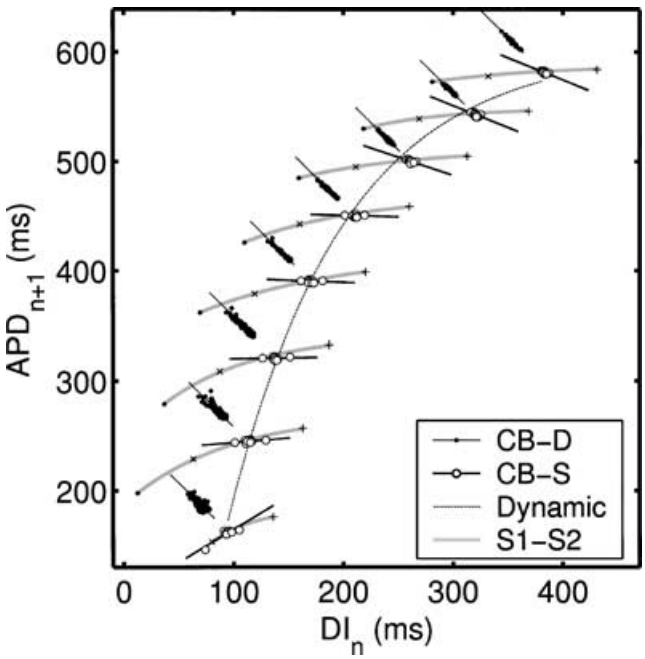

Figure 5. *Restitution portrait showing collection of restitution curves for all basic cycle lengths (BCLs) for the same preparation as for the data shown in Figure 2. At each BCL, there are two CB restitution responses (CB-D and CB-S) and one S1-S2 restitution curve. For these data, BCL was decreased from 950 to 250 ms, with Δ = 100 ms and δ = 50 ms. APD_{n+1} and DI_n are equally scaled to assist visual estimation of slopes.*

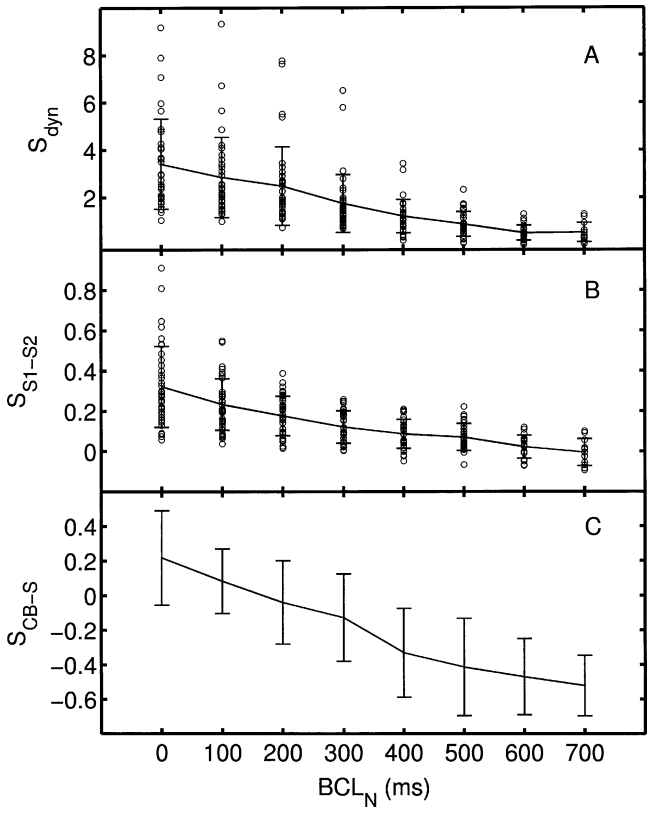

Figure 6. *Mean slopes versus normalized basic cycle length (BCL_N) for all trials. Only BCLs displaying 1:1 behavior are included. Error bars indicate standard deviation. A: Mean $S_{dyn}(^*)$ increases beyond unity as BCL_N decreases. Open circles are slope values. B: Mean $S_{S1-S2}(^*)$ increases yet remains shallow as BCL_N decreases. Open circles are slope values. C: Mean $S_{CB-S}(^*)$ increases from negative to positive values as BCL_N increases. Due to the increased scatter in the S_{CB-S} data, slope values are not shown.*

slightly steeper at shorter BCLs. Its slope $S_{S1-S2}(^*)$ increased from 0.06 at BCL = 950 ms to 0.53 at BCL = 250 ms, where "(*)" indicates that slope is measured at the fixed point. The slope of the CB-S restitution curve at the fixed point $S_{CB-S}(^*)$ changes from negative to positive, increasing from –0.41 to 0.61 through the course of the downsweep.

For quantitative analysis of slope trends over all experiments, BCL was normalized by defining $BCL_N = BCL - BCL_t$, where BCL_t is the shortest BCL in the downsweep with a 1:1 response at steady state. Normalization was performed because transitions from the 1:1 state to 2:1 or 2:2 occurred at different BCLs in different trials.

Figure 6, panels A–C, shows mean $S_{dyn}(^*)$, $S_{S1-S2}(^*)$, and $S_{CB-S}(^*)$, respectively, as a function of normalized BCL (BCL_N) over all experiments for 1:1 responses. This figure shows trends similar to those that are observed by visual inspection of the restitution curve slopes in the restitution portrait of Figure 5. As shown in Figure 6A, the mean slope of the dynamic restitution curve over all experiments steepened beyond unity for $BCL_N < 600$ ms. The average maximal slope at $BCL_N = 0$ was 3.9. We had previously reported similar results ($S_{dyn}(^*) > 1$ for 1:1 responses) with only 10 seconds of pacing at each BCL.[14] The S1-S2 restitution curve remained relatively flat, increasing in slope on average from 0 to 0.32 as BCL_N decreased from 700 to 0 ms (Fig. 6B). The open circles indicating individual slope values show that $S_{S1-S2}(^*)$ sometimes showed marked increase at the shorter BCLs. As can be seen in Figure 5, the slope of the CB-S restitution curve rotated from negative to positive values as BCL was decreased. Over all experiments, the mean value of $S_{CB-S}(^*)$ increased from –0.54 to 0.20 with decreasing BCL_N.

The CB-D responses oscillated about or fell on the BCL-line (slope = –1) in all cases. These responses represent the long-term decrease in APD (illustrated in Fig. 3) termed *accommodation*. For CB-D restitution, constant pacing requires that $APD_n + DI_n = BCL$. Because APD changes slowly due to accommodation, $APD_n \approx APD_{n+1}$ on a beat-to-beat basis, resulting in points that fall on the BCL-line, for a slope always equal to –1.

Restitution Portrait: 2:2 Responses

Most trials yielded a restitution portrait like that shown in Figure 5. However, in 4 of 6 preparations, 2:2T and/or 2:2P responses were seen in some trials. Figure 7A shows an

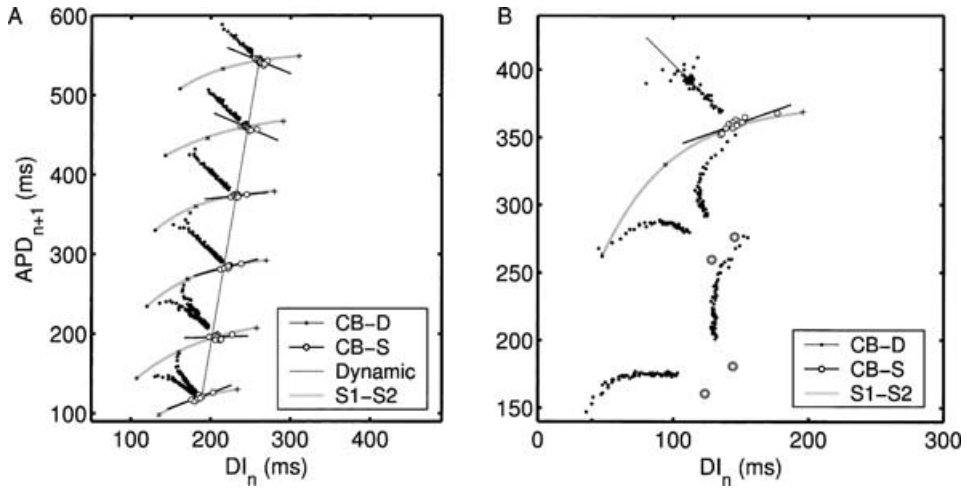

Figure 7. *A: Restitution portrait for an experiment showing transient alternans. Transient alternans is seen in the CB-D response at the shorter basic cycle lengths (BCLs). These responses become 1:1 within step I of the protocol. The first 40 seconds of pacing at each BCL is shown in the CB-D curves. B: Restitution portrait for an experiment showing persistent alternans. In this trial, initial pacing was applied for 120 seconds. The small filled circles represent the first 40 seconds of pacing. The heavy open circles show the response after 120 seconds.*

example of the restitution portrait for a preparation showing 2:2T responses. In this example, the BCL was decreased from 800 to 200 ms with $\Delta = 100$ ms. The steady-state response was 1:1 for BCLs of 800 to 300 ms and 2:1 for a BCL of 200 ms (2:1 response not shown). The transient alternans are seen in the CB-D points that oscillate about the BCL-line. The duration of alternation is greater at the lower BCLs. However, upon continued pacing at each BCL, the magnitude of alternans decreases and APD approaches a 1:1 steady-state within the 60 seconds of initial pacing. Therefore, in the restitution portrait, 2:2T responses appear as two branches that ultimately join on the BCL-line.

For 2:2P responses, the oscillations about the BCL-line persisted for the duration of step I pacing. Therefore, 2:2P responses remain as two separate branches that are symmetric about the BCL-line in the restitution portrait. For these cases, $|\Delta APD_n|$ ranged from 7 to 67 ms after step I pacing; this magnitude of alternation may have decreased with continued pacing. An example of 2:2P responses is shown in Figure 7B. In this particular example, step I pacing was applied for 120 seconds rather than the standard 60 seconds ($\Delta = 100$ ms). Here, alternans persisted for 120 seconds, and $|\Delta APD_n|$ did not decrease between the end of initial recording (40 seconds) and the recording of steady-state data (120 seconds). Thus, although the response was only measured for 120 seconds, the alternans shows no indication of decreasing in magnitude to a 1:1 response.

Slopes during 2:2 responses

During both transient and persistent alternans, the slope formed by all alternating response pairs was approximately unity (1 ± 0.25, mean $\pm$ SD). However, as shown for a representative example in Figure 8, the 2:2 responses did not fall onto either the dynamic restitution curve (dashed line) or the curve resulting from the perturbations to the BCL (gray line). This is not surprising, as others have reported that S1-S2 restitution curves generated during alternans differ depending on whether the S2 stimulus was given after the long or short beat.[29,30] Therefore, slopes $S_{dyn}(^*)$, $S_{S1-S2}(^*)$, and $S_{CB-S}(^*)$ could not be measured during persistent alternans.

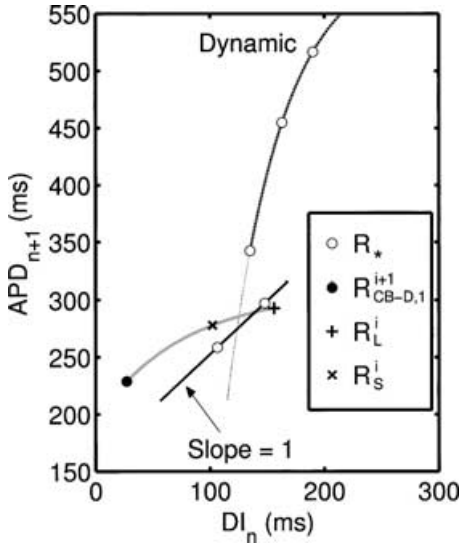

Figure 8. *Restitution curves obtained for an experiment showing persistent alternans. For clarity, CB-D and CB-S responses are not shown. The steady-state responses, R_*, are shown with open circles. For the basic cycle length (i), the steady-state response is 2:2P. These responses R^i_* fall on a line of slope = 1 (solid black line). These points do not coincide with either the dynamic restitution curve (dashed line) or an S1-S2 restitution curve formed by the responses to the long and short perturbations (solid gray line) at that basic cycle length.*

Restitution Curve Slopes and Prediction of Alternans

The slopes of the restitution curves associated with each of the responses 1:1, 2:2T, and 2:2P were examined to assess whether any of the slopes is predictive of alternans. For a one-dimensional dynamical system, the slope at the fixed point gives an indication of the stability of that fixed point. However, as described earlier, slopes during 2:2P responses could not be measured. Therefore, we approximated these slopes by the slope values at the *preceding* BCL. For consistency, this approximation was also used for 1:1 and 2:2T responses.

An example of the use of this approximation in assigning slope values to responses is shown in Figure 9. In this example, the response shown by the small heavy circles, labeled R^B_{CB-D}, was classified as 2:2P. The slopes of the dynamic, S1-S2, and CB-S restitution curves at the fixed point of the preceding BCL ($B+\Delta$), as indicated by the thick lines in Figure 9, were determined and associated with this particular 2:2P response. Responses at all BCLs in all trials were assigned slope values in this manner.

This methodology was used to examine slopes for two cases: (1) steady-state alternans and (2) the *initial* appearance of alternans. To examine steady-state alternans, those responses that were 1:1 at steady state (1:1 and 2:2T) were compared to responses that were 2:2 at steady state (2:2P). Figure 10A shows histogram plots comparing slopes $S_{dyn}(^*)$, $S_{S1-S2}(^*)$, and $S_{CB-S}(^*)$ for the steady-state responses: 1:1 versus 2:2. With 2:2 responses occurring at shorter BCLs, these plots show the same slope trends of Figure 6: shallow yet increasing $S_{S1-S2}(^*)$ with 2:2 responses, steepening $S_{dyn}(^*)$,

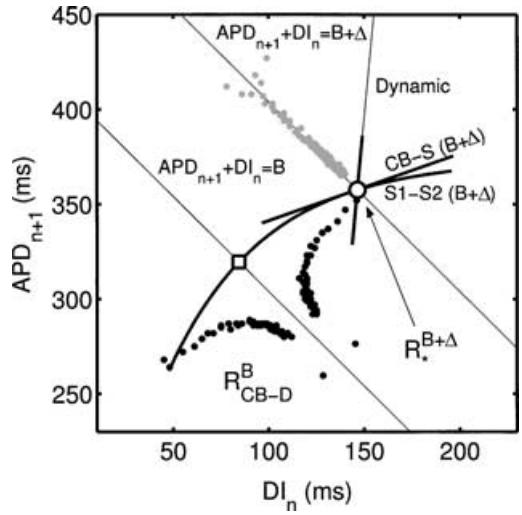

Figure 9. *Slopes are calculated at the fixed point for basic cycle length (BCL) = $B+\Delta$, for the response R^B_{CB-D} at BCL = B (thick dots). The fixed point is indicated by the large open circle. The large open square represents the point at which $S_{S1\text{-}S2}(B)$ was measured. This point marks the intersection of the S1-S2 restitution curve with the BCL-line for the response R^B_{CB-D} ($APD_{n+1}+DI_n = B$).*

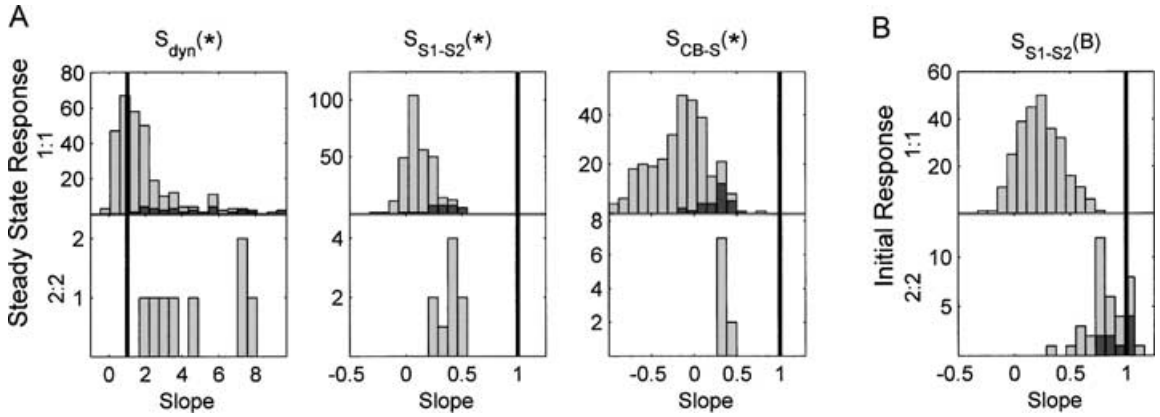

Figure 10. *Histogram plots showing the number of each type of response having a given slope at the preceding basic cycle length (BCL). A: Slopes of the respective restitution curves at the fixed point. Upper panel shows responses that were 1:1 at steady state [1:1 (light bars) and 2:2T (dark bars)]. Lower panel shows responses that were 2:2 at steady state (2:2P). B: S1-S2 restitution curve for the preceding BCL evaluated at its intersection with the BCL-line for the new BCL. Upper panel shows responses that did not initially alternate (1:1). Lower panel shows responses that did initially alternate [2:2T (light bars) and 2:2P (dark bars)]. Dark vertical line indicates slope = 1.*

and shallow yet more positive $S_{CB-S}(*)$. As the lower panels show, none of the restitution-curve slopes alone appears to predict a 2:2P response.

To examine the initial appearance of alternans, those responses showing a 2:2 response immediately after a change in BCL (2:2T and 2:2P) were compared to those that did not alternate (1:1). As shown in Figure 10A, there was no distinction between these two categories for $S_{dyn}(*)$, $S_{S1-S2}(*)$, and $S_{CB-S}(*)$; all slopes were either much greater than 1 ($S_{dyn}(*)$) or much less than 1 [$S_{S1-S2}(*)$, and $S_{CB-S}(*)$].

These results show that slopes at the fixed point of the preceding BCL did not predict alternans for either case: steady state or initial. Possibly, this BCL is too far from the bifurcation point to predict alternans. Therefore, for each of these two cases, an additional estimate also was examined. For the case of steady-state alternans, we used slope trends to extrapolate the slope to the fixed point of the BCL showing the 2:2P response. This extrapolation serves as an upper bound for the slope at the bifurcation point. For each trial showing a 2:2P response, linear fits of $S_{dyn}(*)$, $S_{S1-S2}(*)$, and $S_{CB-S}(*)$ were performed as a function of BCL_N (mean $r = 0.99$, 0.91, and 0.95, respectively). Table 1 shows the values of the extrapolated slopes for each of these trials in parentheses in columns 3 to 5. These upper bounds also do not predict steady-state alternans: for $S_{S1-S2}(*)$, and $S_{CB-S}(*)$ nearly all values are much less than 1; for $S_{dyn}(*)$, the values are much greater than 1.

For the case of initial alternans, we examined the slope of the S1-S2 restitution curve at the preceding BCL but at a different point (not the fixed point). Here, we computed S_{S1-S2} at the intersection of the S1-S2 restitution curve with the BCL-line for the new BCL (B), i.e., the BCL of the response being examined. Figure 9 shows the distinction between this point, $S_{S1-S2}(B)$, determined at the point indicated by the large open square, and $S_{S1-S2}(*)$, indicated by the large open circle. The histograms for $S_{S1-S2}(B)$ are shown in Figure 10B. The upper panel shows slopes for responses classified as 1:1. The lower panel shows slopes for those responses that alternated transiently or persistently (2:2T and 2:2P). Because S1-S2 restitution curves are approximated by an exponential, $S_{S1-S2}(B)$ is steeper than $S_{S1-S2}(*)$, as shown in the figure. Furthermore, the slope $S_{S1-S2}(B)$ approaches unity for the 2:2 responses. Therefore, $S_{S1-S2}(B)$ is the only slope in this study that appears to be predictive of the initial occurrence of alternans.

Comparison with Existing Models of Cardiac Dynamics

In this section, we demonstrate how the restitution portrait can be used to evaluate mapping models of cardiac dynamics. We specifically examine three types of mapping models

TABLE 1

Slopes and Stability Criteria for 2:2P Responses†

Exp. No.	Δ (ms)	$S_{dyn}(*)$‡	$S_{S1-S2}(*)$	$S_{CB-S}(*)$	$S_{S1-S2}(B)$	Criterion (4)	Criterion (8)
1	100	2.17 (2.53)	0.49 (0.58)	0.45 (0.75)	1.02	0.29	0.04
2	100	3.01 (3.48)	0.36 (0.55)	0.35 (0.54)	1.06	0.49	0.24
3	100	8.66 (11.66)	0.39 (0.60)	0.49 (1.02)	0.99	0.57	0.19
4	100	3.83 (4.77)	0.28 (0.31)	0.30 (0.76)	0.88	0.65	0.44
5	100	4.20 (4.89)	0.31 (0.36)	0.35 (0.47)	1.07	0.62	0.37
6	50	9.68 (10.90)	0.42 (0.40)	0.36 (0.43)	0.77	0.56	0.18
7	100	7.08 (7.88)	0.28 (0.30)	0.32 (0.50)	0.89	0.66	0.42
8	50	7.16 (7.89)	0.43 (0.46)	0.37 (0.40)	0.81	0.49	0.16
9	100	3.52 (3.93)	0.54 (0.49)	0.32 (0.35)	0.91	0.38	0.016

†Only experiments showing persistent alternans are included. The slopes of different restitution curves and the stability criteria are calculated at the value of the basic cycle length (BCL) just before the first appearance of persistent alternans. Criteria (4) and (8) are calculated from columns 3–5, i.e., the slopes at the fixed point of the preceding BCL.

‡Values in parentheses indicate extrapolated slope at the next BCL in the downsweep based on linear fit of change in slope with BCL for that experiment.

that differ from each other by the amount of memory they possess. With the incorporation of memory into a mapping model, the criterion for stability can differ from the restitution condition and rate-dependent restitution becomes possible. Because the restitution portrait measures restitution more extensively than the protocols that produce a single restitution curve, it provides a means for more in-depth assessment of rate-dependent restitution. Here, we compare our experimental results with numerical iteration of existing map models using the same perturbed downsweep protocol as in the experiment (presented in the Methods section). The main experimental results that we are comparing to the models are (1) rate-dependent restitution (existence of different restitution curves for different protocols) and (2) long-term accommodation. We also use our experimental data to assess the stability criterion derived from each model.

One-Dimensional Mapping Model Without Memory

The one-dimensional mapping model, first proposed by Guevara et al.,[7] has no memory and describes the APD as a function of only the previous DI in the form of $APD_{n+1} = f(DI_n)$, where f is the restitution curve. It can be seen from Figure 11A that, for such a model, there is only one restitution curve regardless of the pacing protocol: all points fall on $f(DI_n)$. Thus, the memoryless mapping model cannot describe the results of our experiment.

The criterion for the existence of alternans in this mapping model was initially presented by Nolasco and Dahlen,[6] and it states that alternans will occur if the slope of the restitution curve is >1. Recall that this stability criterion is the restitution condition believed by many to apply to cardiac preparations. However, due to the existence of different restitution curves, it is clear that the criterion for stability resulting from this memoryless, one-dimensional model cannot be applied to our experimental results. Indeed, for our data, this conventional wisdom (i.e., the restitution condition) is incorrect whether it is applied to the dynamic, S1-S2, or CB restitution curves (Fig. 10A).

One-Dimensional Mapping Model with Memory

Based on empirical data, Gilmour and collaborators[21] proposed a new type of mapping model to describe their experiments on dog Purkinje fiber. Later, a model of this form was derived analytically[31] from a simplified ionic model of cardiac membrane. This model assumes that the APD depends not only on preceding DI but also on preceding APD so that:

$$APD_{n+1} = F(DI_n, APD_n). \tag{3}$$

The mapping model (3) is still a one-dimensional map because the pacing relation $APD_n + DI_n = BCL$ allows elimination of APD_n from (3). However, the explicit dependence of F on both APD_n and DI_n allows the model to display rate-dependent restitution. Figure 11B presents results of the numerical iteration of the model (3) for the particular form of the function F taken from reference 31. It can be seen from Figure 11B that the dynamic, S1-S2, and CB restitution curves are different in this model, similar to our experimental results. However, there is only a single CB restitution curve for both the dynamic and S1-S2 transients for the mapping model (3), which contradicts our observation of *two different* CB restitution curves: CB-D and CB-S. The absence of the slow monotonic decrease in APD during step I of the protocol, i.e., a separate CB-D restitution response, suggests that the model does not produce long-term accommodation as seen in our experiment.

The criterion for existence of alternans in the mapping model (3) was derived by Tolkacheva et al.[24] It predicts that alternans may exist when:

$$\left|F'\right| = \left|1 - S_{S1-S2} - \frac{S_{S1-S2}}{S_{dyn}}\right| \geq 1. \tag{4}$$

Comparison of the criterion (4) with experimentally observed slopes of different types of restitution curves shows that this criterion is not satisfied. In the histogram of Figure 12A, F' exceeds one for 1:1 responses and decreases for 2:2 responses. The values of F' presented in column 7 of

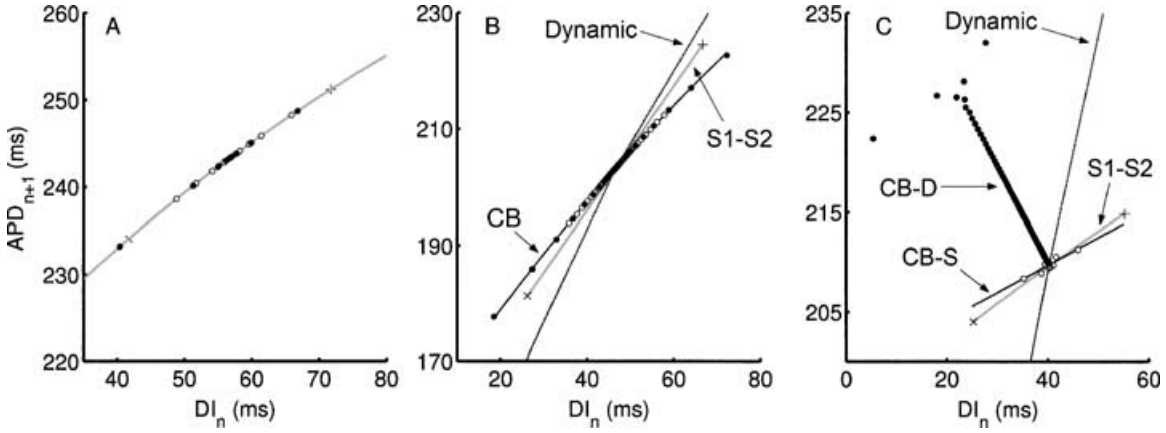

Figure 11. *Results of iteration of mapping models for a single basic cycle length (BCL) using the perturbed downsweep protocol. Symbols for responses: (×) R_S, (+) R_L, (•) R_{CB-D}, (○)R_{CB-S}. A: One-dimensional mapping model without memory $f(DI_n) = A_1 - A_2\ exp(-DI_n/\tau)$ with parameters $A_1 = 300$ ms, $A_2 = 100$ ms, $\tau = 100$ ms, BCL = 300 ms. All points fall on a single curve. B: One-dimensional mapping model with memory (3) for the particular form of the function F taken from reference 31 for typical parameters values and BCL = 250 ms. There are three different restitution curves as a manifestation of short-term memory. Both CB-D and CB-S responses lie along a single CB restitution curve. C: Two-dimensional mapping model with memory (5) with the function $G(DI_n)$ given by expression (6). The parameters are $a_1 = 1{,}500$ ms, $a_2 = 300$ ms, $\tau_1 = 100$ ms, $\tau_2 = 30{,}000$ ms, BCL = 250 ms. There are four different restitution curves as a result of the memory. The CB-D and CB-S responses construct two different CB restitution curves.*

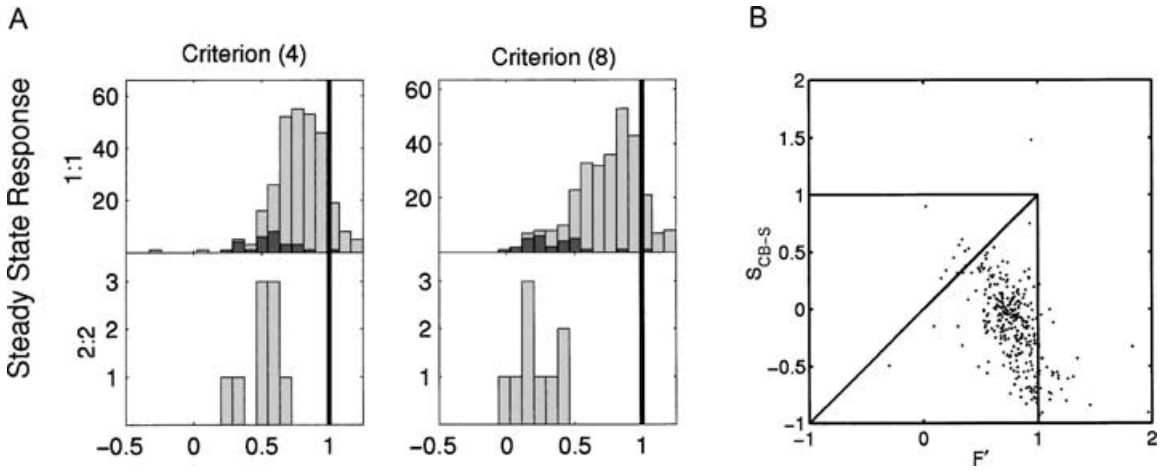

Figure 12. *A: Histograms of criteria (4) and (8) for steady-state responses. Upper panels show the number of 1:1 steady-state responses that have a given value for criterion (4) or (8). Light bars are 1:1 responses; dark bars are 2:2T responses. Lower panels show responses that are 2:2 at steady state (2:2P). B: Plot of S_{CB-S} as a function of stability criterion F′ (4). The map of (3) predicts $F' = S_{CB-S}$. The plot shows that this equality does not hold.*

Table 1 are determined according to criterion (4) for those experiments showing persistent alternans. It can be seen that all of them are well below 0.7.

Another theoretical prediction for the mapping model (3) is that the slope of the CB-S restitution curve S_{CB-S} is equal to F'. In Figure 12B, we plot measured S_{CB-S} as a function of F' as calculated from (4) for all BCLs and experiments. The dots do not fall on a line of slope 1, indicating that the equality, and therefore mapping model (3), does not describe our experimental data.

Two-Dimensional Mapping Model with Memory

Several experimental and theoretical studies[14,20,22,23,32] indicate that longer-term memory effects should be taken into account in order to explain the more complex dynamics found in small cardiac preparations. One formulation for these effects, introduced by Gulrajani,[32] is a memory variable M_n that accumulates during the APD and dissipates during the DI. A specific mapping model with this formulation for memory was proposed by Chialvo et al.[20] and is given by:

$$APD_{n+1} = (1 - M_{n+1})G(DI_n) \tag{5A}$$

$$M_{n+1} = \{1 - (1 - M_n)\exp[-APD_n/\tau_2]\}\exp[-DI_n/\tau_2], \tag{5B}$$

where:

$$G(DI_n) = a_1 - a_2\exp[-DI_n/\tau_1]. \tag{6}$$

The parameters a_1, a_2, τ_1, and τ_2 are tissue dependent. It was shown by Tolkacheva et al.[33] that the mapping model (5) can be rewritten in the following form:

$$APD_{n+1} = F(DI_n, APD_n, DI_{n-1}), \tag{7}$$

i.e., it incorporates dependence on one more previous beat in comparison to the mapping model (3).

Figure 11C shows the results of numerical iteration of the two-dimensional mapping model (5) at a single BCL. There are four different restitution curves (dynamic, S1-S2, and two CB restitution curves) in this model, similar to our experimental results. The long-term behavior (the CB-D restitution curve) is governed by the parameter τ_2, which was chosen to be on the same order as the accommodation in the experiment (~20–30 s). The full restitution portrait for this model, shown in Figure 13, has many qualitative similarities to our experimental restitution portraits: four distinct curves at each BCL, CB-D slope is consistently –1, CB-S slope rotates from negative to positive, and the S1-S2 slope remains relatively flat. However, despite very good qualitative agreement with the experimental results (Fig. 5), the quantitative agreement is poor. For example, it is impossible to obtain a dynamic restitution curve as steep as those seen in experiments for the functional form of $G(DI_n)$ given in (6) when τ_2 is sufficiently large to produce long-term accommodation on the same time scale as that of our experimental preparation.

For mapping models of the form of (7), the general criterion for existence of alternans was derived by Tolkacheva et al.[33] It predicts that alternans exist when:

$$1 - S_{S1-S2} - \frac{S_{S1-S2}}{S_{dyn}} + \frac{S_{S1-S2}(1 - S_{dyn})}{S_{dyn} - S_{S1-S2}} \times \left(1 - S_{S1-S2} - \frac{S_{S1-S2}}{S_{dyn}} + S_{CB-S}\right) \leq -1. \tag{8}$$

This expression was evaluated using the experimentally measured slopes of the different restitution curves and is presented for different response classifications in Figure 12A. Table 1 (column 8) presents this value for those experiments displaying persistent alternans. It can be seen that this criterion does not hold for our experimental results.

It is important to note that the slopes should be calculated at the onset of alternans to rigorously test the stability criteria. The primary purpose of this experiment was not to test the stability criterion; thus, the onset of alternans was not determined exactly. Therefore, the values given in Table 1 are an approximation of the values at the transition point. However, values for criteria (4) and (8) calculated with the upper bounds for slopes shown in parentheses in Table 1 are also less than 0.7 and 0.4, respectively (data not shown). In addition, the trends in the plots of Figures 10A and 12A support the failure of (4) and (8) to predict alternans.

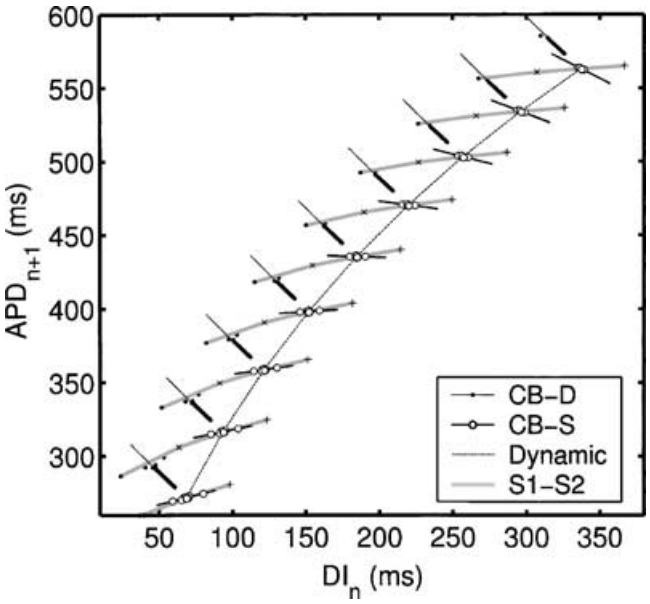

Figure 13. *Restitution portrait generated by iteration of mapping model (5) with the $G(DI_n)$ as given in (6). The parameters are $a_1 = 1{,}500$ ms, $a_2 = 300$ ms, $\tau_1 = 100$ ms, $\tau_2 = 30{,}000$ ms. BCL was decreased from 900 to 340 ms, $\Delta = 70$ ms, $\delta = 30$ ms. Note the qualitative similarities between this restitution portrait and that shown in Figure 5.*

Discussion

Restitution Portrait

In this study we have modified the pacing protocol suggested by Tolkacheva et al.[24] by adding a measurement of the initial transient after a change in BCL. We implemented this new perturbed downsweep protocol in an in vitro frog heart preparation. This protocol allowed simultaneous observation of all of the restitution curves typically used to assess stability of the 1:1 response in the restitution portrait: a dynamic restitution curve, segments of S1-S2 restitution curves at each BCL, and two types of CB restitution responses, the CB-D and CB-S.

When these curves are plotted together in a restitution portrait, the distinctions between them are emphasized. In particular, S1-S2 and dynamic restitution curves measure the immediate and steady-state responses to a change in BCL, respectively. With the additional measurement of CB restitution, we can also observe the transient responses, which illustrate that restitution has both a fast and slow component. The CB-D restitution curve demonstrates the response to a sustained change in BCL (slow component), while the CB-S shows the response following a brief perturbation in BCL (fast component). The initial oscillation of the CB-D responses also demonstrates the fast component of restitution, similar to the CB-S restitution (Fig. 3). In examining the long-term decay of the CB-D responses along the BCL-line, it also becomes apparent how the slope of the dynamic restitution curve will be affected by pacing for an insufficient duration at each BCL.

The restitution portrait is expected to vary for different experimental preparations. The memory properties of a preparation will affect the shape of individual restitution curves and the degree of rate dependence. For example, the preparation presented here had a very steep dynamic restitution curve compared to those reported for some other preparations.[8,10] A preparation with a shallower dynamic restitution curve may produce a restitution portrait more like that shown in Figure 13. Also, the restitution portraits of larger preparations may differ from those in a 3×5 mm piece of ventricle because electrotonic effects and conduction velocity restitution may alter APD dynamics.[34] Some preparations would also be expected to yield regionally and/or transmurally varying restitution portraits due to underlying APD differences. However, the qualitative features resulting from the fast and slow components of restitution should be retained for any type of experimental preparation, even though the details of the restitution portrait may vary.

Restitution Condition Revisited

The restitution condition is the basis for the conventional wisdom regarding the onset of electrical instability in cardiac tissue. However, it is based on a model that does not reproduce the experimentally observed cardiac dynamics. Therefore, as demonstrated by the restitution portrait, the restitution condition is not valid: it does not account for rate dependence and effects of accommodation. In this respect, our data agree with several recent studies that have questioned the validity of the restitution condition due to the exclusion of memory[14,19,23,34] as well as spatial considerations[15,34] in underlying models. Thus, our simple intuitive understanding of the origin of alternans must be replaced by a more comprehensive picture.

The restitution portrait can help us to take the first step in this direction because it allows visualization of the evolution of alternans and the role of memory in this process. Figure 7, panels A and B, demonstrate that if alternans appears immediately after a change in BCL, the effects of long-term accommodation tend to decrease the magnitude of alternation over time, which may ultimately result in a 1:1 behavior. The mechanism of this evolution can be interpreted by using a model proposed by Watanabe and Koller.[22] In that study, memory was investigated by measuring shifts in the restitution curve induced by multiple extrastimuli. The restitution curves measured therein were similar to the S1-S2 restitution curve as defined here; however, they were not measured during a steady-state S1-S1 response but rather during accommodation. Watanabe and Koller found that these restitution curves shifted downward with an increasing number of extrastimuli at a shorter BCL. For a sufficient number of extrastimuli, their resulting restitution curve would be equivalent to the S1-S2 restitution curve that we have defined here.

In abruptly changing the BCL from one step to the next in the perturbed downsweep protocol (e.g., from BCL1 to BCL2), the initial occurrence of alternans appears to be linked to the S1-S2 restitution curve measured for BCL1 (Fig. 10B). If the slope of the S1-S2 restitution curve at its intersection of the BCL-line for BCL2 ($S_{S1-S2}(B)$) is ≥ 1, the response will oscillate upon changing BCL. If we assume subsequent responses to be determined by a downward shifting restitution curve as proposed by Watanabe and Koller, the intersection of this curve with the BCL-line will move to the right with each new stimulus, where the restitution curve is shallower. Therefore, with sustained pacing, the slope at the intersection point with the BCL-line may become <1 and the alternans will convert to a 1:1 response. Whether alternans will persist depends on both the slope of the S1-S2 restitution curve $S_{S1-S2}(B)$ and the action of memory. Even if $S_{S1-S2}(B)$ does

not indicate persistent alternans, transient alternation in APD of sufficient duration may still be arrhythmogenic. Therefore, $S_{S1-S2}(B)$ may provide a marker for the onset of electrical instability.

Validity of the Existing Mapping Models

The restitution portrait is a means to test the existing mapping models by showing both long- and short-term responses in the different restitution curves. The CB restitution curves, which are not measured typically, are a particularly revealing aspect of the restitution portrait. In our analysis, we have examined the implications of the existence of the observed restitution curves for mapping models with varying degrees of memory. In this way, this protocol allows a more comprehensive test of model validity than testing the stability criterion alone.

Observation of rate-dependent restitution necessitates incorporation of some degree of memory in a mapping model. Mapping model (3), which has one-beat memory, does show rate-dependent restitution but not produce all of the experimentally observed restitution curves. Theoretical predictions of model (3) are also not met: $F' \neq S_{CB-S}$, and neither appears to indicate stability.

Mapping model (5), which is a special case of (7), includes one additional memory term: DI_{n-1}. This slight increase in memory produces the long-term effects necessary to produce two CB restitution responses. However, model iteration does not produce quantitative agreement with the experimentally observed steep dynamic restitution. A different functional form of $G(DI_n)$ may result in a better fit for our data. The stability criterion (8), which is independent of the functional form of the mapping, does not hold for our results. Thus, our results suggest that higher dimensional effects must be taken into account in order to produce a mapping model with a stability criterion that applies more accurately to preparations showing memory. The roles of the restitution curves for such a mapping model remain to be determined. However, we have shown that models that are only *slightly* more complex allow for qualitative agreement with experimental temporal cardiac dynamics. Therefore, further investigation of such moderately complex phenomenologic models may give rise to clinically useful concepts, replacing the restitution condition, and serve as an aid for drug targeting.

Study Limitations

The results presented here were collected from only one site on the myocardium. However, even in a small preparation, spatial factors such as conduction velocity restitution and cell-to-cell coupling are present and may influence the presence of alternans,[34] as well as the appearance of the restitution portrait. To study the extent of these factors, a logical extension of this work would be to examine the spatial variation of the restitution portrait with a larger preparation using multisite recording techniques, such as optical mapping.

Another limitation of our study is that the perturbed downsweep protocol used here was not optimized to examine stability. The long-term accommodation observed in our preparations necessitated at least a full minute of pacing at each BCL to reach steady state. Thus, in order to maintain stable impalements for the duration of the experiment (10–15 min), coarse step sizes were used in most cases, making it difficult to examine the stability criterion and slopes of the S1-S2 and CB-S restitution curves right at the bifurcation to alternans. This was further complicated by the fact that the time to reach steady state for persistent 2:2 responses was much greater (on the order of several minutes) than the 60 seconds of S1 pacing used in this protocol. This phenomenon, termed *critical slowing down,* is a common observation in nonlinear dynamical systems.[35] Thus, a modification of the existing protocol should be developed specifically for collecting data needed for the stability criteria.

Examining stability was further limited by the low incidence of persistent alternans observed in our study. Although previous experiments in our laboratory have produced similar rates of prevalence of alternans in in vitro studies of paced bullfrog myocardium,[14] Savino et al.[36] report a higher incidence of alternans in a different animal model. Their study used the in vivo toad heart and the whole perfused ventricle, and APD was measured using a suction monophasic action potential (MAP) electrode. Several factors may have contributed to their routine observation of alternans, including species, tissue perfusion method, larger preparation, and mechanical action of the MAP electrode. In the future, to study alternans more extensively, a modification of our experimental setup may be needed.

References

1. Mines GR: On dynamic equilibrium in the heart. J Physiol Lond 1913:46:349-383.
2. Karma A: Electrical alternans and spiral wave breakup in cardiac tissue. Chaos 1994;4:461-472.
3. Smith JM, Clancy SM, Valeri R, Ruskin JN, Cohen RJ: Electrical alternans and cardiac electrical instability. Circulation 1988;77:110-121.
4. Rosenbaum DS, Jackson LE, Smith JM, Garan H, Ruskin JN, Cohen RJ: Electrical alternans and vulnerability to ventricular arrhythmias. N Engl J Med 1994;330:235-241.
5. Pastore JM, Girouard SD, Laurita KR, Akar FG, Rosenbaum DS: Mechanism linking T-wave alternans to the genesis of cardiac fibrillation. Circulation 1999;99:1385-1384.
6. Nolasco JW, Dahlen RW: A graphic method for the study of alternation in cardiac action potentials. J Appl Physiol 1968;25:191-196.
7. Guevara MR, Ward G, Shrier A, Glass L: Electrical alternans and period-doubling bifurcations. IEEE Comp Cardiol 1984;562:167-170.
8. Koller ML, Riccio ML, Gilmour RF Jr: Dynamic restitution of action potential duration during electrical alternans and ventricular fibrillation. Am J Physiol 1998;275:H1635-H1642.
9. Qu Z, Weiss JN, Garfinkel A: Spatiotemporal chaos in a simulated ring of cardiac cells. Phys Rev Lett 1997;78:1387-1390.
10. Riccio ML, Koller ML, Gilmour RF Jr: Electrical restitution and spatiotemporal organization during ventricular fibrillation. Circ Res 1999;84:955-963.
11. Gilmour RF: A novel approach to identifying antiarrhythmic drug targets. Drug Discovery Today 2003;8:162-167.
12. Weiss JN, Garfinkel A, Karagueuzian HS, Qu Z, Chen P-S: Chaos and the transition to ventricular fibrillation: A new approach to antiarrhythmic drug evaluation. Circulation 1999;99:2819-2826.
13. Gilmour RF: Electrical restitution and ventricular fibrillation: Negotiating a slippery slope. J Cardiovasc Electrophysiol 2002;13:1150-1151.
14. Hall GM, Bahar S, Gauthier DJ: Prevalence of rate-dependent behaviors in cardiac muscle. Phys Rev Lett 1999;82:2995-2998.
15. Banville I, Gray RA: Effect of action potential duration and conduction velocity restitution and their spatial dispersion on alternans and the stability of arrhythmias. J Cardiovasc Electrophysiol 2002;13:1141-1149.
16. Gilmour RF, Otani NF, Watanabe MA: Memory and complex dynamics in cardiac Purkinje fibers. Am J Physiol 1997;272(4 Pt 2):H1826-H1832.
17. Elharrar V, Surawicz B: Cycle length effect on restitution of action potential duration in dog cardiac fibers. Am J Physiol 1983;244:H782-H792.
18. Rosen MR: What is cardiac memory? J Cardiovasc Electrophysiol 2000;11:1289-1293.
19. Fenton FH, Evans SJ, Hastings HM: Memory in an excitable medium:

a mechanism for spiral wave breakup in the low-excitability limit. Phys Rev Lett 1999;83:3964-3967.
20. Chialvo DR, Michael DC, Jalife J: Supernormal excitability as a mechanism of chaotic dynamics of activation in cardiac Purkinje fibers. Circ Res 1990;66:525-545.
21. Otani, NF, Gilmour RF Jr: Memory models for the electrical properties of local cardiac systems. J Theor Biol 1997;187:409-436.
22. Watanabe MA, Koller ML: Mathematical analysis of dynamics of cardiac memory and accommodation: Theory and experiment. Am J Physiol 2002;282:H1534-H1547.
23. Fox JJ, Bodenschatz E, Gilmour RF: Period-doubling instability and memory in cardiac tissue. Phys Rev Let 2002;89:138101-138104.
24. Tolkacheva EG, Schaeffer DG, Gauthier DJ, Krassowska, W: Condition for alternans and stability of the 1:1 response pattern in a "memory" model of paced cardiac dynamics. Phys Rev E 2003;67:031904.
25. Boyett MR: An analysis of the effect of rate of stimulation and adrenaline on the duration of the cardiac action potential. Pflügers Arch 1978;377:155-166.
26. Gibbs CL, Johnson EA, Tille J: A quantitative description between the area of rabbit ventricular action potentials and the pattern of stimulation. Biophys J 1963;3:344:458.
27. Boyett MR, Jewell BR: Analysis of the effects of changes in rate and rhythm upon electrical activity in the heart. Prog Biophys Mol Biol 1980:36:1-52.
28. Franz MR, Swerdlow CD, Liem LB, Schaefer J: Cycle length dependence of human action potential duration *in vivo*: Effects of single extrastimuli, sudden sustained rate acceleration and deceleration, and different steady-state frequencies. J Clin Invest 1988;82:972-979.
29. Pastore JM, Rosenbaum DS: Spatial and temporal heterogeneities of cellular restitution are responsible for arrhythmogenic discordant alternans. Circulation 1999;100(Suppl S):257.
30. Rubenstein DS, Lipsius SL: Premature beats elicit a phase reversal of mechanoelectrical alternans in cat ventricular myocytes: A possible mechanism for reentrant arrhythmias. Circulation 1995;91:201-214.
31. Tolkacheva EG, Schaeffer DG, Gauthier DJ, Mitchell CC: Analysis of the Fenton-Karma model through approximation by a one-dimensional map. Chaos 2002;12:1034-1042.
32. Gulrajani RM: Computer simulation of action potential duration changes in cardiac tissue. IEEE Comp Cardiol 1987;244:629-632.
33. Tolkacheva EG, Romeo MM, Guerraty M, Gauthier DJ: Condition for alternans and its control in a two-dimensional mapping model of paced cardiac dynamics. Phys Rev E 2004;69:031904.
34. Cherry EM, Fenton FH. Suppression of alternans and conduction blocks despite steep APD restitution: Electronic, memory and conduction velocity restitution effects. Am J Physiol Heart Circ Physiol 2004 Jan 29 [Epub ahead of print].
35. Strogatz SH: *Nonlinear Dynamics and Chaos*. Reading, PA: Addison-Wesley Publishing, 1994.
36. Savino GV, Romanelli L, Gonzalez DL, Piro O, Valentinuzzi ME: Evidence for chaotic behavior in driven ventricles. Biophys J 1989;56:273-280.